Acta Crystallographica Section B
Structural Science
ISSN 0108-7681

Reversible pressure-induced structure changes in turbostratic BN–C solid solutions

Vladimir L. Solozhenko* and Oleksandr O. Kurakevych

LPMTM-CNRS, Université Paris Nord, F-93430 Villetaneuse, France

Correspondence e-mail: vls@lpmtm.univ-paris13.fr

Received 13 June 2005
Accepted 4 August 2005

The results obtained by Rietveld analysis and numerical modeling of B–C–N layered clusters with various types of lattice defects explain the evolution of diffraction patterns of turbostratic graphite-like BN–C solid solutions which are experimentally observed at room temperature at pressures up to 30 GPa. Above 20 GPa a reversible diffusionless transformation of the initial turbostratic structure takes place, giving a high-pressure phase formed by close-packed buckled layers having a diamond-like structure.

1. Introduction

The structure formed by layers which are parallel and equidistant, but random in translation parallel to the layer, with rotation about the normal is usually called a turbostratic (or one-dimensionally disordered) structure. Interest in these structures was stimulated by intensive studies of carbon black in the middle of the last century (Biscoe & Warren, 1942; Franklin, 1950, 1951). The quantitative theory of X-ray diffraction by the random layer lattice has been developed by Warren (1941) and describes the diffraction patterns of one-dimensionally disordered graphite-like phases under ambient pressure (Biscoe & Warren, 1942; Franklin, 1950). Turbostratic structures have recently attracted attention because many newly synthesized graphite-like phases (Kaner *et al.*, 1987; Hubaček & Sato, 1995; Kawaguchi *et al.*, 1996; Shirasaki *et al.*, 2000; Solozhenko *et al.*, 2002) can be excellent precursors for the synthesis of advanced superhard materials (Solozhenko *et al.*, 2001; Onodera *et al.*, 2001; Solozhenko, 2002; Solozhenko *et al.*, 2004).

The phase transitions of turbostratic carbon and boron nitride take place at very high (> 2000 K) temperatures and lead to ordered graphite-like structures (Kurdyumov & Pilyankevich, 1979). Room-temperature pressure-induced transformations of turbostratic phases have not been reported previously.

Recently, Solozhenko *et al.* (2001) studied *in situ* phase transitions of graphite-like BC_2N (g-BC_2N) up to 30 GPa and 3000 K using a diamond–anvil cell and angle-dispersive X-ray diffraction with synchrotron radiation. The diffraction patterns observed under compression at room temperature indicate the changes in the structure of the starting turbostratic phase. The similarity of the patterns taken above 25 GPa to that of diamond (absence of 001 line, symmetry of 10 line[1] and its shift towards the 111 diamond reflection)

[1] Following Warren's approach (Warren, 1941), we use two Miller indices to denote the two-dimensional reflections.

Table 1
Initial and resulting pseudo-unit cells (triclinic syngony, $P1$ space group).

Lattice parameters: $\alpha = \beta = \gamma = 90^\circ$.

Cell	Description	Lattice parameters (Å)	Atomic coordinates
g_0	Graphite layer	a = 4.3371 b = 2.5041	$(x_{g0}(i), y_{g0}(i), 0)$ x_{g0} = [1/3 2/3 1/6 5/6] y_{g0} = [0 0 $\frac{1}{2}$ $\frac{1}{2}$]
d_0	Diamond layer	a = 4.3686 b = 2.5222 (c = 12.354)	$[x_{d0}(i), y_{d0}(i), z_{d0}(i)]$ $x_{d0} = x_{g0}$ $y_{d0} = y_{g0}$ z_{d0} = $[-z_1\ 0\ 0\ -z_1]$ z_1 = 0.0416
g_1	Randomly buckled graphite layer	a = 4.3371 b = 2.5041 (c = 33.331)	$[x_{g0}(i), y_{g0}(i), f_4(x,y,z)]$
g_2	Graphite layer with diamond-like buckling	a = 4.3371 b = 2.5041 (c = 12.354)	$(x_{g0}, y_{g0}, k{\cdot}z_{d0})$ $k \in [0; 1]$
G_0	Graphite (10 layer cell)	a = 4.3371 b = 2.5041 c = 33.331	$[x_{g0}(i), y_{g0}(i), z_1(j)]$ $[x_{g0}(i) + \frac{1}{3}, y_{g0}(i), z_2(j)]$ z_2 = [0 0.2 0.4 0.6 0.8]] z_3 = [0.1 0.3 0.5 0.7 0.9]
D_0	Diamond (six-layer cell)	a = 4.3686 b = 2.5222 c = 12.354	$[x_{d0}(i), y_{d0}(i), z_{d0}(i) + z_4(j)]$ $[x_{d0}(i) + \frac{1}{3}, y_{d0}(i), z_{d0}(i) + 1/6 + z_4(j)]$ $[x_{d0}(i) + 2/3, y_{d0}(i), z_{d0}(i) + 2/6 + z_4(j)]$ z_4 = [0 1/2]
G_1	G_0 cell with layers displaced in relation to each other along the a and b axes	a = 4.3371 b = 2.5041 c = 33.331	$[x_{g0}(i) + f_1(z), y_{g0}(i) + f_2(z), z_5(j)]$ $z_5 = z_2 \cup z_3$ f_1, f_2 described in text
G_2	G_0 cell with layers displaced in relation to each other along the a, b and c axes	a = 4.3371 b = 2.5041 c = 33.331	$[x_{g0}(i) + f_1(z), y_{g0}(i) + f_2(z), z_5(j) + f_3(z)]$ f_3 described in text
G_3	G_1 cell with randomly buckled layers	a = 4.3371 b = 2.5041 c = 33.331	$[x_{g0}(i) + f_1(z), y_{g0}(i) + f_2(z), z_5(j) + f_4(x,y,z)]$ f_4 described in text

allows us to make a proposal about the pressure-induced reconstruction of the sp^2 structure of g-BC_2N into the diamond-like sp^3 structure.

Pressure-induced martensitic phase transformations have previously only been observed at room temperature for highly ordered graphite-like structures of carbon and boron nitride (Kurdyumov & Pilyankevich, 1979; Ueno *et al.*, 1992; Britun & Kurdyumov, 2000). In the case of turbostratic g-BC_2N, the transformation cannot be implemented by any of the known crystallographic mechanisms (Britun & Kurdyumov, 1999) as the complete one-dimensional disordering of the initial phase rules out the martensitic mechanism for the transformation. The low temperature precludes the operation of the diffusion processes within the framework of the diffusion-reconstructive mechanism.

In the present work the behavior of turbostratic BN–C solid solutions has been studied up to 30 GPa and at room temperature using X-ray diffraction with synchrotron radiation. With the aim of explaining the observed evolution of the diffraction patterns, Rietveld analyses of the experimental patterns and simulated diffraction patterns of layered finite-size B–C–N clusters with lattice defects of various types were carried out.

2. Materials

Our starting materials were nanopowders of turbostratic graphite-like BN–C solid solutions of various stoichiometry (BC_2N, BC_4N and BCN), which were synthesized by the simultaneous nitridation of boric acid and the carbonization of saccharose in molten urea followed by annealing in nitrogen at 1770 K (Hubaček & Sato, 1995). The diffraction patterns of all materials have broad diffraction lines (001, 10, 002 and 11) which are typical of turbostratic structures. Interlayer spacings for BC_2N, BC_4N and BCN were found to be 3.63 (2), 3.64 (2) and 3.66 (3) Å, respectively, while the a parameters have the same value of 2.48 (2) Å.

3. Experimental

Phase transitions of graphite-like BN–C solid solutions were studied up to 30 GPa at room temperature using a large-aperture membrane-type diamond–anvil cell and angle-dispersive X-ray diffraction at beamline ID30, European Synchrotron Radiation Facility. The experimental setup is described elsewhere (Solozhenko *et al.*, 2001). The samples were loaded, without a pressure medium, in the 100 µm diameter hole drilled in a rhenium gasket of thickness 250 µm preindented down to 55 µm. Pressure was determined from the calibrated shift of the ruby R_1 fluorescence line (Mao *et al.*, 1986). The high-brilliance synchrotron radiation from a two-phased undulator was set to a wavelength of 0.3738 (1) Å using a channel-cut Si(111) monochromator. The patterns were collected using an on-line image-plate FastScan detector (Thoms *et al.*, 1998). Correction of the two-dimensional diffraction images for spatial distortions and integration of the Debye–Scherrer rings were performed using FIT2D software (Hammersley, 1995).

4. Calculation methods

The approximation of absolutely flat and equidistant layers that are randomly displaced and turned relative to each other [which is used in the Warren approach (Warren, 1941) to depict turbostratic defects in layered structures] allows the diffraction patterns of graphite-like structures at ambient pressure to be adequately described. However, this approximation does not allow the diffraction patterns observed under pressure to be described. This is likely due to the generation of defects of other types in addition to the turbostratic ones.

4.1. Rietveld method

According to Warren (1941), the expression for the intensity of diffracted radiation I contains three main multipliers, which are F^2, the square of the structure factor corresponding to the 'ideal' lattice, the two-dimensional interference function and the term describing the randomness of the interlayer orientation

$$I = F^2 \frac{\sin^2(\pi/\lambda)(\mathbf{s}-\mathbf{s}_0)N_1\mathbf{a}}{\sin^2(\pi/\lambda)(\mathbf{s}-\mathbf{s}_0)\mathbf{a}} \frac{\sin^2(\pi/\lambda)(\mathbf{s}-\mathbf{s}_0)N_2\mathbf{b}}{\sin^2(\pi/\lambda)(\mathbf{s}-\mathbf{s}_0)\mathbf{b}} \times \sum_{m_3} \exp[(2\pi i/\lambda)(\mathbf{s}-\mathbf{s}_0)(m_3\mathbf{c} + rnd(m_3)\mathbf{a} + rnd(m_3)\mathbf{b})] \sum_{m_3}{}^{*}.$$

As the aim of the present work is to explain the behavior of the intensities of the main X-ray reflections in relation to each other, the Rietveld method (Rietveld, 1969) may be applied: this allows the effect of various types of distortion of the original 'ideal' lattice on the intensities of the 001 and 10 lines to be estimated. Although this method has been developed for periodic structures and does not allow the full analysis of disordered structures, it easily reveals changes in the layer structure (assuming that 'randomness' in the mutual layer orientation of the original and refined structures remains the same). The relative intensities of the changes in $F^2(hk0)$ and $F^2(00l)$ change. We have used the graphite-like cell G_0 (all cells are listed in Table 1) consisting of ten flat layers as the inital pseudo-unit cell for Rietveld analysis.

We used four additional functions that correspond to the structural defects to describe the initial and final pseudo-unit cells. The function $f_1(x,y,z)$ characterizes the buckling and takes values from 0 (flat layers g_0) up to 0.5139/c (diamond-like layers d_0); three variables point to the mutual independence of the atom displacements within a layer. $f_2(z)$ and $f_3(z)$ characterize the layer stacking faults and take the values from the unit interval [0, 1], while the variable z shows that the function takes the same value for all the atoms of a given layer. The function $f_4(z)$ describes the layer displacement from the ideal position. The *PowderCell* program (Kraus & Nolze, 1996 was used for the refinement of the atomic coordinates.

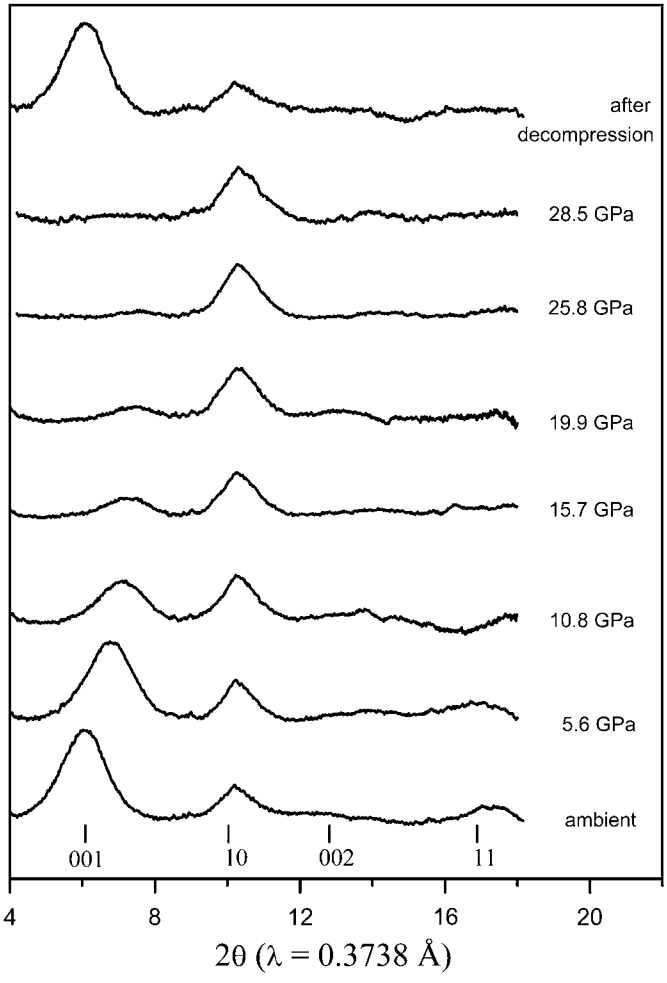

Figure 1
Diffraction patterns of turbostratic g-BC_2N taken at room temperature and various pressures.

4.2. *Ab initio* calculation of powder patterns of B–C–N layered clusters

The comprehensive analysis of disordered layered structures is possible only within the framework of the direct calculation of diffraction patterns for finite-sized clusters with preset defects. The clusters have been constructed employing the sandwich model with alternating graphite-like carbon and BN layers, as suggested by Hubaček & Sato (1995). The calculations were made using the Debye (1915) equation, which relates the intensity of the scattered radiation to the scattering angle

$$I(s) = \left(\frac{1+\cos^2 2\theta}{2}\right) \sum_p \sum_q f_p f_q \frac{\sin sr_{pq}}{sr_{pq}},$$

where $s = 4\pi\sin\theta/\lambda$, f_p and f_q are the atomic scattering factors of atoms p and q, and r_{pq} is the distance between atoms p and q. The atom positions are given by a vector

$$\mathbf{R}^n_{m_1m_2m_3} = \mathbf{R}_{m_1m_2m_3} + \mathbf{r}_n + \mathbf{R}_{sl} + \mathbf{R}_d + \mathbf{R}_b,$$

where $\mathbf{R}_{m_1m_2m_3} = m_1\mathbf{a} + m_2\mathbf{b} + m_3\mathbf{c}$ is the translation vector, $\mathbf{r}_n$ is the basis vector of the atom n in a unit cell of ideal two-dimensional lattices, $\mathbf{R}_{sl} = rnd(m_3)\mathbf{a} + rnd(m_3)\mathbf{b}$ is the slip vector of layer m_3 along a and b crystallographic axes, $\mathbf{R}_d = rnd(m_3)\mathbf{c}$ is the vector corresponding to the variation of spacing between the m_3 and $(m_3 - 1)$ layers, $\mathbf{R}_b = rnd(m_1, m_2, m_3, n)\mathbf{c}$ is the vector that defines the buckling of layer m_3 (specifies the shift along the c axis of each n atom in the m_1m_2 cell). The layers have been rotated using the rotation operator $\mathbf{R}_z(\theta)$ with $\theta = rnd(m_3)$. We have calculated the diffraction patterns for clusters containing from 2000 to 5000 atoms. To construct clusters we used a structural unit comprising the diamond-like pseudo-unit cell D_0, which is formed by six buckled layers with an interlayer spacing of 2.059 Å which corresponds to d_{111} of diamond. The simulation was performed using the *MATLAB* program package (The MathWorks, 2002).

5. Results and discussion

5.1. X-ray data: reversible changes of powder pattern shape

Our experiments have shown that a pressure increase at room temperature is accompanied by a pronounced decrease in the intensity of the 00*l* lines of the initial graphite-like BN–C solid solutions (Fig. 1). Thus, upon compression up to 20 GPa, the intensity of the strongest 00*l* line of graphite-like BC_2N decreases by a factor of 6, and at 25 GPa this line almost disappears. This cannot be explained by the pressure-induced preferred orientation of the crystallites, because the diffraction plane normal was parallel to the axis of the diamond–anvil cell, with which the more compressible *c* direction tends to align, and increases in the 00*l* line intensities are expected in this case. At the same time, a change of the diffraction pattern in the region of the 10 asymmetrical line of the turbostratic structure is observed. The intensity of scattering in this region increases, the profile of the line becomes increasingly symmetrical and its maximum shifts towards 2.07 Å, which is close to the line positions observed for the 111 reflections of diamond and cubic BN. The reconstruction proceeds at room temperature and completely terminates at pressures of the order 25 GPa. A similar evolution of diffraction patterns under pressure has been observed for all turbostratic graphite-like B–C–N phases.

Our *in situ* experiments have shown that changes in the diffraction patterns of turbostratic BN–C solid solutions are fully reversible up to pressures of the order 30 GPa. This indicates that the total disappearance of the 001 lines under pressure is caused not by the destruction of the layered structure, but by an abrupt change in the interlayer spacing from 2.7 Å (compressed turbostratic phase) to 2.1 Å (spacing between buckled layers forming a diamond-like structure) or by some specific change of layer structure that could weaken the inter-layer reflections. Thus, what we are observing is a phase transformation of turbostratic g-BC_2N into a high-pressure phase, which proceeds over a wide pressure range and terminates at 25–30 GPa.

5.2. Rietveld analysis: variation of interlayer spacing and random buckling

The Rietveld refinement of the *z* coordinates of each graphite-like layer in the G_1 cell reveals that the experimentally observed $J_{001} \geq J_{10}$ relation between line intensities in diffraction patterns of turbostratic g-BC_2N up to 10 GPa can be satisfactorily explained assuming that the initial structure is disordered with respect to interlayer spacings (G_2 cell, see Fig. 2). A similar type of disordering has been previously observed for partially graphitized carbon (Franklin, 1951). In our case, it is likely that in the course of the g-BC_2N compression, a non-uniform change in the relative orientation of the layers takes place, which is accompanied by a non-uniform approach between layers, giving rise to a layered structure with various interlayer spacings. The calculated patterns and experimental data are in good agreement, while the deviation of the layer position along the *c* axis has not exceeded 0.1 Å [according to Franklin (1951), the corresponding value for carbon phases is *ca* 0.1 Å].

The $J_{001} < J_{10}$ relation, which is experimentally observed at pressures above 10 GPa, can be explained assuming that the layers are buckled. Fig. 3 shows the diffraction pattern obtained by the Rietveld refinement of the *z*-coordinates of each atom in the G_1 cell. The pattern corresponds to a structure with 'randomly' buckled layers (cell G_3). It should be noted that in the framework of the Rietveld formalism an increase in J_{10} stems from the appearance of additional intense lines with $l = 0$ near the tenth line of the initial turbostratic phase, which points to a decrease in symmetry of the pseudo-unit cell under pressure. However, the 001 line still remains intense. Thus, the assumption of 'random' buckling is not

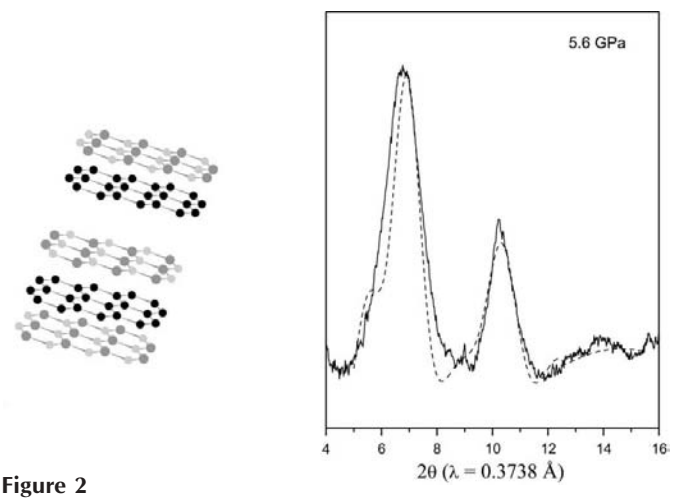

Figure 2
Hypothetical structure and diffraction patterns of turbostratic g-BC_2N at 5.6 GPa (the solid line indicates the experimental pattern, the dashed line the pattern obtained from a Rietveld refinement of the *z*-coordinates of flat layers).

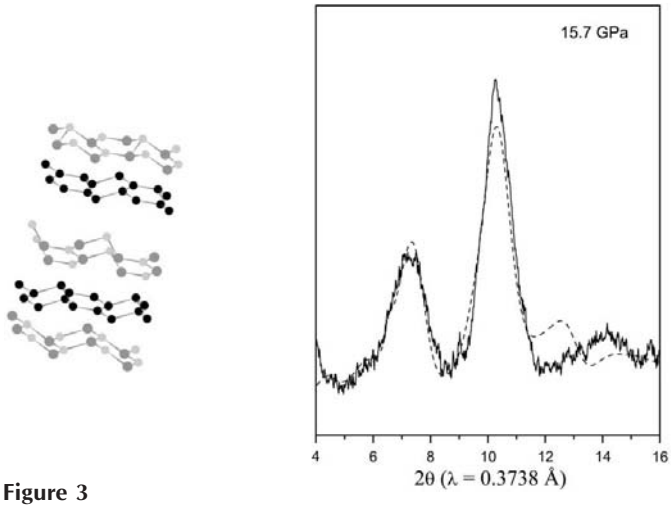

Figure 3
Hypothetical structure and diffraction patterns of turbostratic g-BC_2N at 15.7 GPa (the solid line shows the experimental pattern, the dashed line indicates the pattern obtained from a Rietveld refinement of the *z*-coordinates of individual atoms).

Table 2
Turbostratic structures.

Lattice parameters: $\alpha = \beta = \gamma = 90°$.

Structure	Description	Lattice parameters (Å)
T_{g0}	Turbostratic structure with g_0 layers stacked along the c axis	a = 4.3371 b = 2.5041 c = 3.4†
T_{g1}	Turbostratic structure with g_1 layers stacked along the c axis	a = 4.3371 b = 2.5041 c = 3.0†
T_{g2}	Turbostratic structure with g_2 layers stacked along the c axis	a = 4.3371 b = 2.5041 c = 2.7†
T_{d0}	Turbostratic structure with d_0 layers stacked along the c axis	a = 4.3686 b = 2.5222 c = 2.1†

† In general, the parameter may vary from 2.1 up to 3.4.

sufficient to explain the complete disappearance of the 001 line in the patterns of turbostratic g-BC_2N at high pressures.

5.3. Simulation of diffraction patterns: ordered buckling and stepwise change of interlayer spacings

The results of the simulation of diffraction patterns have shown that for a compressed turbostratic structure, the change-over from flat to buckled layers is accompanied by a decrease in the 001 line intensity and a rise in the 10 line intensity. However, with the ordered buckling (g_2 cell), a total disappearance of the 001 line is not observed as well as in the case of the 'random' buckling (g_1 cell). The only possible explanation for the disappearance of the 001 line is a discontinuous change of interlayer distance under pressure. When considering the discontinuous change, all the layers do not collapse at the same pressure. Below 25 GPa, the 001 line is always present and moves as expected when the pressure increases. Above 15 GPa, the abrupt change in interlayer spacings at a given pressure occurs only between certain pairs of layers. The fraction of compressed turbostratic graphite-like structure decreases with pressure. Finally, the total disappearance of the initial phase is observed at *ca* 25 GPa.

In order to describe the experimental diffraction patterns at pressures above 25 GPa, which are characterized by an intense band in the region of the 111 line of diamond-like phases and by the absence of bands in the region of other lines (*220, 311*), we have simulated patterns of layered structures with interlayer spacings of 2.1 Å corresponding to d_{111} of the diamond-like phases. The disturbance of the ordering along the c axis of the diamond-like buckled layers of a diamond-like structure (layers built on the base of d_0 and g_2 cells) tends to increase the intensity of the 10 line of the resulting disordered layered structure compared with other lines at higher angles (Fig. 4).

5.4. Model of high-pressure behavior of turbostratic phase

For ordered graphite-like phases, the buckling of layers under pressure is a necessary stage of the martensitic transformation at room temperature (Britun & Kurdyumov, 2000; Mao *et al.*, 2003). Thus, Mao *et al.* (2003) have recently reported that buckling of the graphite layers under hydrostatic compression occurs at lower pressures than the formation of the dense phase and is accompanied by splitting of the 100 and 110 in-plane reflections of the initial phase and by line broadening. In a similar manner, buckling of the layers should proceed in the course of the compression of turbostratic structures (T_{g0}, see Table 2). Under pressure the layers approach each other and the interlayer interaction intensifies (the role of the repulsive forces increases), with the result that the atoms tend to occupy the energetically preferred positions by displacement relative to each other. Finally, at some sufficiently high pressure buckling occurs (T_{g1} or T_{g2} structures). The abrupt approach between buckled layers then gives rise to a structure similar to T_{d0} (see Fig. 5), corresponding to patterns taken at pressures above 20 GPa. This may be caused by reaching some critical value of buckling, which allows the layers to approach each other, or by changes in the mutual orientation of layers owing to rotation and displacement. The change in mutual orientation occurs because of the increasing role of repulsive forces between the layers, leading to other types of one-dimensional disorder [*i.e.* different types of

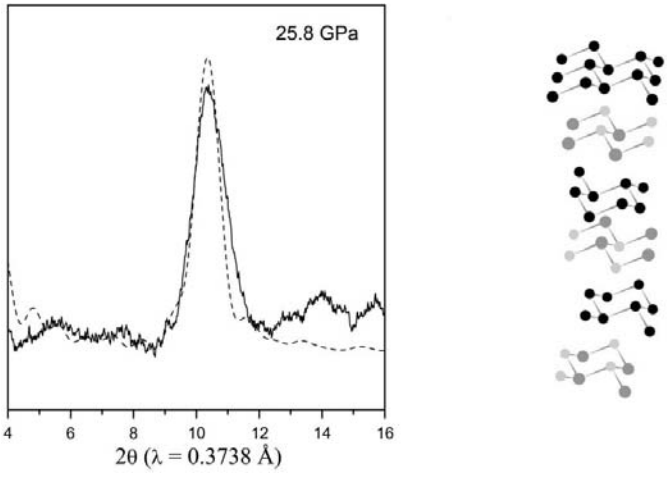

Figure 4
Calculated diffraction pattern of the one-dimensionally disordered structure, which is formed by properly buckled layers (dashed line), and the experimental pattern taken at 25.8 GPa (solid line).

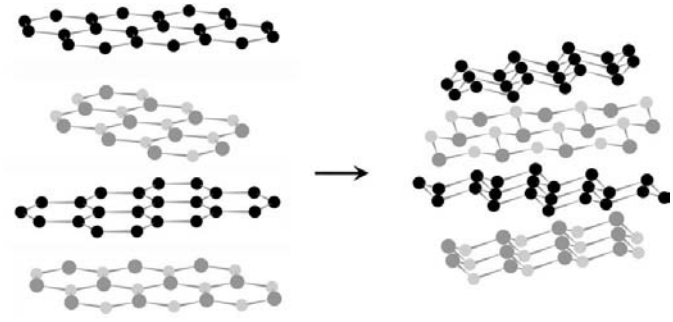

Figure 5
Structures of the initial turbostratic g-BC_2N and the high-pressure phase formed by close-packed buckled layers.

'$rnd(m_3)$' functions describing the lattice defects] than those found in the original turbostratic phase. As the diffraction patterns corresponding to the initial turbostratic phase completely recover their original shape as soon as the pressure is released, it may be concluded that the layers remain in the region of the elastic forces over the whole range of pressures under study and the formation of covalent bonds between the layers does not occur. According to the first-principles analysis of a continuous transition path from rhombohedral graphite to diamond (Fahy *et al.*, 1986), no inter-layer bonding occurs until the inter-atomic distance is within 10% of the C—C bond length in diamond. This result is consistent with our model of the disordered high-pressure phase.

6. Conclusions

In the course of compression at room temperature, all turbostratic graphite-like B–C–N phases show similar behavior that is indicative of the phase transformation associated with a discontinuous change of interlayer distance. The suggested mechanism includes the buckling (sp^2-to-sp^3 transition) and change of the mutual orientation of layers. The initial turbostratic phase passes into the disordered high-pressure phase consisting of close-packed buckled layers with a diamond-like structure (Fig. 5). The transformation is fully reversible and the formation of covalent bonds between the layers does not occur.

We thank Drs D. Andrault and M. Mezouar for their assistance in the high-pressure experiments. Special thanks go to Dr M. Hubaček for supplying the turbostratic BN–C samples. DAC experiments were carried out during the beamtime allocated to proposal HS-1693 at ID30, ESRF. This work was partially supported by the National Science Foundation Grant No. DMR-0102215.

References

Biscoe, J. & Warren, B. E. (1942). *J. Appl. Phys.* **13**, 364–371.
Britun, V. F. & Kurdyumov, A. V. (1999). *Materialovedenie*, **6**, 26–31 (in Russian).
Britun, V. F. & Kurdyumov, A. V. (2000). *High Press. Res.* **17**, 101–111.
Debye, P. (1915). *Ann. d. Physik B*, **46**, 809–823.
Fahy, S., Louie, S. G. & Cohen, M. L. (1986). *Phys. Rev. B*, **34**, 1191–1199.
Franklin, R. E. (1950). *Acta Cryst.* **3**, 107–121.
Franklin, R. E. (1951). *Acta Cryst.* **4**, 253–261.
Hammersley, A. (1995). *FIT2D.* ESRF, Grenoble, France.
Hubaček, M. & Sato, T. (1995). *J. Solid State Chem.* **114**, 258–264.
Kaner, R. B., Kouvetakis, J., Warble, C. E. & Sattler, M. E. (1987). *Mater. Res. Bull.* **22**, 399–404.
Kawaguchi, M., Kawashima, T. & Nakajima, T. (1996). *Chem. Mater.* **8**, 1197–1201.
Kraus, W. & Nolze, G. (1996). *J. Appl. Cryst.* **29**, 301–303.
Kurdyumov, A. V. & Pilyankevich, A. N. (1979). *Phase Transformations in Carbon and Boron Nitride*, pp. 91–95. Kiev: Naukova Dumka (in Russian).
Mao, H. K., Xu, J. & Bell, P. M. (1986) *J. Geophys. Res.* **91**, 4673–4676.
Mao, W. L., Mao, H., Eng, P. J., Trainor, T. P., Newville, M., Kao, C., Heinz, D. L., Shu, J., Meng, Y. & Hemley, R. J. (2003). *Science*, **302**, 425–427.
Onodera, A., Matsumoto, K., Hirai, T., Goto, T., Motoyama, M., Yamada, K. & Kohzuki, H. (2001). *J. Mater. Sci.* **36**, 679–684.
Rietveld, H. M. (1969). *J. Appl. Cryst.* **2**, 65–71.
Shirasaki, T., Derre, A., Menetrier, M., Tressaud, A. & Flandrois, S. (2000). *Carbon*, **38**, 1461–1467.
Solozhenko, V. L. (2002). *High Press. Res.* **22**, 519–524.
Solozhenko, V. L., Andrault, D., Fiquet, G., Mezouar, M. & Rubie, D. C. (2001). *Appl. Phys. Lett.* **78**, 1385–1387.
Solozhenko, V. L., Dubrovinskaia, N. A. & Dubrovinsky, L. S. (2004). *Appl. Phys. Lett.* **85**, 1508–1510.
Solozhenko, V. L., Solozhenko, E. G. & Lathe, C. (2002). *J. Superhard Mater.* **24**, 95–96.
The MathWorks, Inc. (2002). *MATLAB*, Version 6.5 R13. The MathWorks, Inc., USA
Thoms, M., Bauchau, S., Häusermann, D., Kunz, M., LeBihan, T., Mezouar, M. & Strawbridge, D. (1998). *Nucl. Instrum. Methods A*, **413**, 175–184.
Ueno, M., Hasegava, K., Osima, R. & Onodera, A. (1992). *Phys. Rev. B*, **45**, 10226–10230.
Warren, B. E. (1941). *Phys. Rev. B*, **59**, 693–698.